Applied Catalysis B: Environmental 95 (2010) 169–178

Contents lists available at ScienceDirect

Applied Catalysis B: Environmental

journal homepage: www.elsevier.com/locate/apcatb

Preferential photodegradation of contaminants by molecular imprinting on titanium dioxide

Dovrat Sharabi, Yaron Paz *

Department of Chemical Engineering and the Russell-Berrie Nanotechnology Institute, Technion, Haifa, Israel

ARTICLE INFO

Article history:
Received 27 September 2009
Received in revised form 14 December 2009
Accepted 17 December 2009
Available online 28 December 2009

Keywords:
Titanium dioxide
Molecular imprinting
Photocatalysis
DIMP
DEHMP

ABSTRACT

The photocatalytic degradation of organic contaminants on titanium dioxide is basically non-selective. While this seems at first glance to be an advantage, this is not the case when a stream containing low concentrations of highly toxic substances together with high concentrations of low toxic organics has to be treated. A method for obtaining preferential degradation by means of preparation of molecularly imprinted photocatalyst is presented hereby. The method is demonstrated with two model compounds simulating the nerve gas sarin: diisopropyl methylphosphonate (DIMP) and diethylhydroxy methylphosphonate (DEHMP).

An improvement by a factor of 3–4 in the mineralization rates was observed upon using the imprinted substrates. This enhancement in photocatalytic rates cannot be explained by the modest growth in the surface area (not more than 20–30%), hence it can be concluded that the enhancement resulted from the conformity between the target molecules and the molecular cavities on the imprinted sites. This conclusion is further supported by the lower extent of enhancement upon degrading benzene and heptane.

Of particular interest is the fact that substrates that were imprinted with DEHMP were found to be very effective in the degradation of the homolog DIMP. This observation suggests the use of molecules having good affinity to the matrix as a means to obtain high surface concentration of molecular active sites, thus detouring the problem of aggregation that might arise in cases where the target contaminants have low affinity to the matrix. Another benefit is the possibility of using non-toxic homolog molecules for constructing the imprinted photocatalyst. This benefit is in particular important when designing a photocatalyst for WMD warfare agents, as in the case of sarin.

1. Introduction

Recent years have shown an increasing interest in photocatalysis. Titanium dioxide is often considered to be the photocatalyst of choice for water, air and surface decontamination due to its low cost, high stability, low toxicity and high photoefficiency when compared with other photocatalysts.

Being based on the strong oxidation potential of the hydroxyl radicals formed on the catalyst surface, TiO_2 photocatalysis can be expected to have very low selectivity [1]. Indeed, the degradation rate of molecules having comparable adsorpticity was found to be quite similar [2]. This lack of sensitivity to the type of contaminants seems to be benevolent at first glance. However, poor selectivity also implies that the photocatalyst does not differentiate between highly hazardous contaminants and organic contaminants of low toxicity. This shortcoming is further aggravated by the fact that while many low toxicity contaminants can be degraded by biological means, many of the highly hazardous materials are non-biodegradable.

Preferential degradation can be obtained by manipulating the adsorption of the contaminants on the photocatalyst's surface. One way to achieve it is by controlling the surface's electric charge [3]. The isoelectric point of titanium dioxide is approximately at pH 6.5 [4], hence pH values higher than 6.5 are favorable for the adsorption of positively charged contaminants, while pH values lower than 6.5 are favorable for adsorption of negatively charged contaminants. Nevertheless, the specificity of this method is very low, not to mention the fact that most contaminants are neutral. Another way to obtain specificity could be based on modifying the titanium dioxide surface with organic molecules that might physisorb specific target molecules [5], however, these organic molecules, located on the photocatalyst surface, are expected to be

* Corresponding author at: Department of Chemical Engineering, Technion-Israel Institute of Technology, Technion City, 32000 Haifa, Israel. Tel.: +972 4 8292486; fax: +972 4 8295672.
E-mail address: paz@tx.technion.ac.il (Y. Paz).

0926-3373/$ – see front matter © 2009 Elsevier B.V. All rights reserved.
doi:10.1016/j.apcatb.2009.12.024

easily attacked by the oxidizing species formed on the photocatalyst's surface.

A different approach ("Adsorb & Shuttle") for obtaining high preferentiability was proposed a few years ago [6]. The core of this approach was the construction of robust, immobile organic molecular recognition sites (MRS) on inert substrates, located on, or in the vicinity of the photocatalyst. These covalently bound self-assembled molecules physisorb the target molecules selectively. Once physisorbed, the target molecules surface-diffuse from site to site towards the interface between the inert domains and the photocatalytic domains, where they are destroyed.

Since the molecular recognition sites are organic, care had to be taken to examine their possible destruction by oxidizing species out-diffusing from the titanium dioxide domains. Indeed, it was found that such oxidizing species can destroy organic molecules anchored on oxide surfaces as far as 40 μm away from the photocatalytic domains [7]. In contrast, self-assembled monolayers on metallic domains such as platinum or gold were found to be stable [8], enabling their use in specific micrometer-size systems designed especially for the degradation of 2-methynaphthoquinone [9], or diisopropyl methylphosphonate (DIMP) [10].

The printing of molecules onto matrices during the preparation process of the matrices, following by the removal of the imprinting molecules to yield cavities having the size and structure of the imprinting molecules was proposed already 60 years ago [11], when enhanced adsorption of alkyl orange on imprinted silica gel was reported. Nevertheless, the interest in the method was very modest until recently, when imprinting of molecules onto polymeric matrices (MIPs) [12,13] was realized as an analytical tool for detecting a variety of molecules such as herbicides [14], proteins [15], and drugs [16].

Sol–gel prepared oxides seem to be most appropriate for molecular imprinting due to their higher rigidity, thermal stability and surface area in comparison with polymers. Indeed, imprinting into silica gel was utilized for the purposes of sensing [17,18], separation [19], and catalysis [20,21].

Imprinting onto TiO_2 matrices was first introduced by Kunitake and co-workers [22], who demonstrated saturated binding of azobenzene carboxylic acid on thin films of titanium dioxide that were overcoated on Quartz Crystal Microbalance (QCM) electrode. The capability to induce specific adsorption was soon followed by the development of sensors detecting a variety of molecules by diverse detection techniques. Examples include peptides [23], microorganisms [24], and L-glutamic acid [25] by QCM, chloroaromatic acids by a Field Effect Transistor (FET) [26], benzenediol [27], parathion [28] and acetaminophen [29] by cyclic voltammography and 2,4-dinitrotoluene [30] by the cyclic surface polarization impedance method.

Despite the large number of publications on photocatalysis by TiO_2, not much is found in the literature on the use of imprinted titanium dioxide for the purpose of photocatalytic decontamination of air and water (Fig. 1), with the exception of imprinting of salicylic acid [31] and diethyl phthalate [32] on a TiO_2-core and aluminum doped silica shell particles. This fact can be explained by the high temperatures required for the phase transition from the amorphous inactive phase, obtained by common sol–gel procedures, into the photoactive anatase phase (>300 °C). These high temperatures, which are around the evaporation/burning temperatures of the templating molecules are likely to prevent the formation of imprinted titanium dioxide if indeed a common sol–gel process is used. It is for this reason, that only procedures by which the anatase is formed at low temperatures could be considered for the present work, aiming at using imprinted titanium dioxide for the photocatalytic degradation of diisopropyl methylphosphonate (DIMP) and diethylhydroxy methylphosphonate (DEHMP) (Fig. 2).

Our interest in the photocatalytic degradation of DIMP and DEHMP stems from their use as simulants for the nerve gas sarin (O-isopropyl methylphosphonate). Sarin is a member of the organophosphonates family of which many members are used as pesticides. The importance of finding secure and efficient ways to degrade sarin is evidenced through the diversity of studies dedicated for its destruction, utilizing the techniques of biodegradation [33], combustion [34], pyrolysis [35], catalysis [36] and photocatalysis [37,38]. Of these techniques, photocatalysis seems to be the most promising for cases of low level pollution in air, as might occur when the nerve gas is distributed in urban areas, where it might be physisorbed first on construction materials, from where it might be released for a relatively long time. In these cases, pre-painting large surfaces such as walls, roads, tarmacs and the like with photocatalytic paint may provide a solution that may assist in the recovery and rehabilitation of the damaged areas. Indeed, the photocatalytic degradation of another stimulant, dimethyl methylphosphonate (DMMP) was thoroughly studied [37–39]. It is for this reason that sarin simulants were chosen to demonstrate the feasibility of using imprinted photocatalysts for enhancing the photodegradation of specific contaminants in air.

2. Experimental

2.1. Preparation of powdered titanium dioxide

Preparation of titanium dioxide by sol–gel methods often requires elevated temperatures (above 275 °C) needed in order to evaporate and burn organic residues and to form the photocatalytic anatase phase. However, applying such temperatures

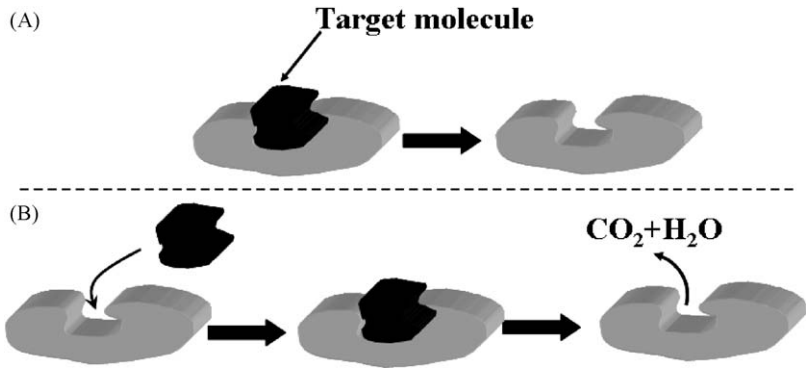

Fig. 1. Photocatalysis by an imprinted photocatalyst: (A) preparation of photocatalyst and (B) use of photocatalyst.

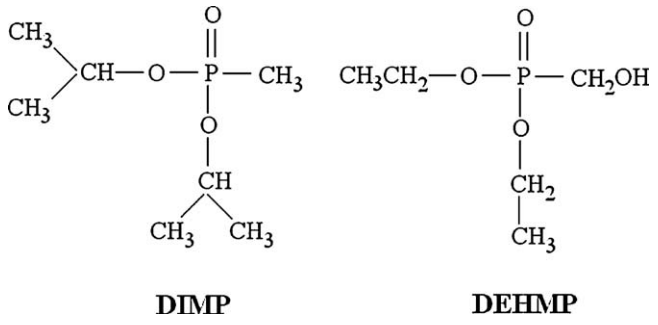

Fig. 2. The imprinted molecules.

during the preparation stage might evaporate or burn also the imprinted molecules and might alter any formed cavities. For this reason a low temperature procedure for the preparation of anatase phase titanium dioxide is preferred.

All powders presented in this manuscript were prepared by adapting the technique of Yamabi and Imai [40] who used aqueous solution of titanyl sulfate ($TiOSO_4$) to form titanium dioxide at low temperatures. According to this method, the crystalline phase (anatase, rutile, or amorphous) of the obtained titania is controlled by the concentration of the $TiOSO_4$ as well as by the initial pH. 5.87 ml of 0.03 M $TiOSO_4$ solution (prepared by diluting a commercially available mother liquor containing 15% $TiOSO_4$ by weight in diluted sulfuric acid (Aldrich)) were mixed with 1.43 ml of concentrated HCl (32% by weight). The mixture was stirred for 1 h at room temperature to give a pH of 1.3. Fine tuning of the pH was done by introducing minute amounts of ammonium hydroxide (NH_4OH). The mixture was then transferred to a flask connected with a water-circulating condenser. The flask was heated to 60 °C for 24 h; then allowed to cool to room temperature. White precipitants were obtained. The precipitates were then separated by vacuum filtration, washed with water and dried overnight in a vacuum oven at 60 °C.

The imprinted TiO_2 powders were prepared in a manner similar to that of the non-imprinted powders. Two types of imprinting molecules were used: diisopropyl methylphosphonate (DIMP, Alfa Aesar) and diethylhydroxy methylphosphonate (DEHMP, Aldrich). First, a solution of HCl and $TiOSO_4$ (0.03 M, 5.876 ml) was prepared as described above. Then, DIMP (0.006 M, 275 μl) or DEHMP (0.006 M, 225 μl), which corresponded to a TiO_2/phosphonate molar ratio of approximately 5:1, was introduced into the aqueous mixture under stirring. The mixture was stirred at room temperature until reaching a pH of 1.3 (approximately 1 h), heated to 60 °C for 24 h, and cooled down to room temperature. The obtained precipitants were separated by vacuum filtration, washed and dried as described for the non-imprinted powder. The templating molecules were removed from the TiO_2 matrix by heat treatment at 420 °C for 3 h that took place right after the drying step.

2.2. Characterization

Both types of samples (imprinted and non-imprinted) were characterized by a variety of methods. The crystalline phase of the powders was identified by X-ray diffractometry (Phillips) utilizing CuKα radiation. Average grain sizes were calculated from the broadening of the (1 0 1) XRD peak using the Scherrer equation, $[L = K\lambda/(\beta \cos(\theta))]$, where L is the crystalline typical length, K is a unit cell geometry dependent constant whose value is typically 0.89, λ is the wavelength of the X-ray irradiation (0.154 for CuKα radiation), β is the full-width-half-maximum of the peak and θ is the Bragg angle.

The surface of the particles was observed using Scanning Electron Microscope (SEM, JEOL5400). All samples were gold-coated by evaporation prior to scanning. The surface area of the TiO_2 samples was estimated by the BET adsorption isotherms of nitrogen at 77 K using an ASAP 2010 machine (Micrometrics). Care was made to de-gas the samples at 200 °C prior to measuring.

Phosphorous nuclear magnetic resonance (^{31}P NMR) was used to investigate the interactions between the TiO_2 and the incorporated phosphonates. ^{31}P NMR was performed to TiO_2/DIMP and TiO_2/DEHMP samples as well as to pure liquid DIMP and DEHMP. Measurements of solid samples were carried out on a Chemagnetics/Varian 300 MHz NMR spectrometer, whereas single pulse excitation measurements of liquid samples were recorded on a Bruker AM-500 machine at 202.5 MHz. Chemical shifts (in ppm) are reported relative to orthophosphoric acid ($\delta = 0.0$) in D_2O.

2.3. Photocatalysis measurements

The photocatalytic measurements were performed with 1 in. × 3 in. glass slides, coated with TiO_2 by a "doctor's blade" technique. To prevent possible inaccuracies in the photocatalytic evaluation due to variations in the thickness of the different samples, care was taken to assure that the films that were used were optically thick (approximately 15 μm). Here, the penetration depth of UV light into titanium dioxide is in the order of 1 μm, hence all impinging photons were actually absorbed at the outer part of all samples regardless of the precise thickness of the films. The samples were prepared by stirring and ultrasonicating of a concentrated (1 g per ml of water) suspension of titanium dioxide, spreading 800 μl of the suspension on the glass slides and drying in an oven for 10 min at 70 °C.

The photodegradation measurements were done in a closed cylindrical glass vessel (40 cm^3), containing two 1.5 in. KBr windows, that enabled FTIR transmission-mode measurements. Each experiment used one slide, coated with either an imprinted or a non-imprinted titanium dioxide film. Once closed, 0.01 ml of DIMP, DEHMP, benzene or heptane was injected into the cell through a septum. Evaporation and adsorption kinetics were then constantly monitored until steady state was reached. Then the cell was illuminated by a low intensity (365 nm, 0.2 mW cm^{-2}) UV light that penetrated into the reactor through the glass opposite to the photocatalyst slide. IR spectra were taken periodically, without opening the cell.

3. Results

3.1. Characterization

The TiO_2 powders, prepared at low temperatures as described above, were characterized by SEM, XRD, BET, and XPS. Fig. 3 presents the SEM images of non-imprinted particles as well as particles imprinted with molecules of DEHMP. As portrayed in the figure, both types of particles were very similar, i.e. spherically shaped, with an average diameter of 0.8–1.3 μm. This was also the case for DIMP-imprinted particles. Evidently, the introduction of the imprinting molecules during the preparation of the particles did not have a noticeable effect on the shape and size of the particles as probed at a micrometer scale.

The crystal structure of the particles in the filtrate (i.e. prior to any treatment) was determined by powder X-ray diffraction. Fig. 4 presents the XRD pattern of both types of particles (non-imprinted and DEHMP-imprinted) revealing the same XRD pattern, indexed as belonging to the anatase phase. The same phase was found also for the DIMP-imprinted particles. The crystalline size was calculated from the width of the (1 0 1) peak at $2\theta = 25.25°$, using the Scherrer equation. An average diameter of 6 nm was calculated for both types of particles. This diameter is significantly smaller than the particles' diameter (Fig. 3), indicating that each particle is comprised of a large number of crystallites. No pronounced effect of the imprinted

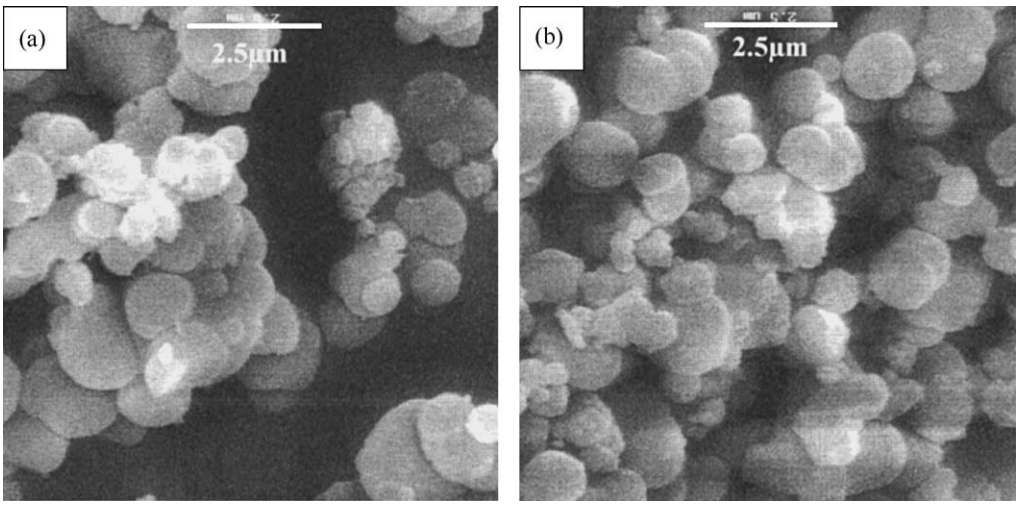

Fig. 3. SEM images of the powders: (A) non-imprinted TiO_2 and (B) TiO_2 imprinted with DEHMP.

molecules on the crystalline phase and size as well as on the micron-scale morphology of the particles could be observed.

The specific surface areas of the various samples, as deduced from the linear part of Brunnauer, Emmett and Teller (BET) isotherm plots are presented in Table 1. The average specific surface area of the particles made by the titanyl sulfate procedure was around 160 m^2/g prior to the heat treatment stage and 145 m^2/g following heat treatment. This 9% reduction in the specific surface area can be considered very mild as it is only slightly above the experimental error. This reduction in the surface areas is attributed to the collapse of the mesoporous framework and to thermal induced crystal growth. It is noteworthy that the specific surface area of imprinted powders prior to heat treatment was not significantly different from that of the non-imprinted samples. Nevertheless, following heat treatment the specific surface area of the non-imprinted powder was lowered by 15% and 21% than that of the DEHMP and DIMP-imprinted powders, respectively. This might imply that to some extent the imprinted phosphonates act to inhibit the collapse of the mesoporous framework and crystal growth.

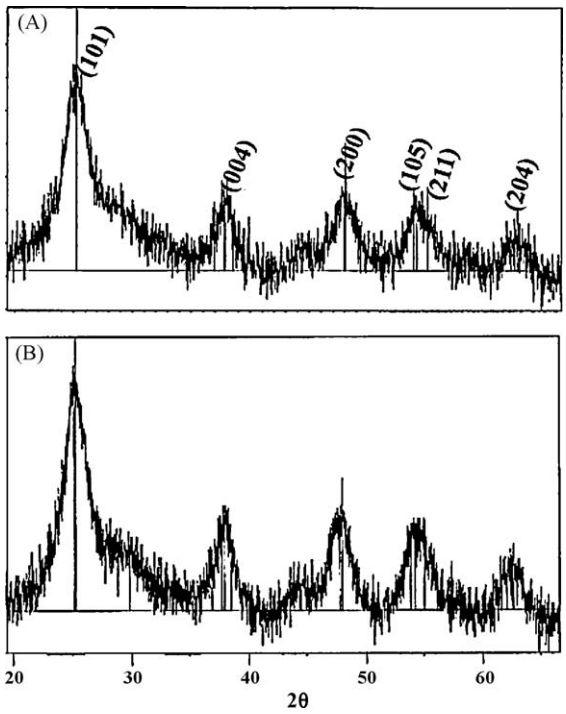

Fig. 4. The XRD pattern of particles formed in the absence of imprinted molecules (upper trace) and upon imprinting with DEHMP (lower trace). Peaks are indexed according to known peaks of anatase.

XPS measurements were taken for TiO_2/DEHMP prior to and following heat treatment. Two types of measurements were recorded, representing the atomic ratio in the particles' bulk as well as at their surfaces. Results are summarized in Table 2. As expected, the dominant elements were oxygen (60–64 at.%) and titanium (16–19 at.%). A relatively high (8–20) atomic percentage of carbon was observed. Some of it originated from contamination, as often found in XPS measurements, and some of it represented the imprinting molecules, hence disappeared following heat treatment. The atomic percentage of phosphorous was approximately 2%. About 50% of it was removed from the surface during the heat treatment. The ratio between oxygen and titanium atoms was approximately 3.3–3.6, higher than the stoichiometric ratio, most likely reflecting adsorbed oxygen and hydroxyls [41] as well as the presence of sulfate ions and phosphates. That sulfate ions present in the particles is evidenced also from the presence of sulfur, which

Table 1
BET specific surface area (m^2/g) of the various particles prepared by the low temperature titanyl sulfate method, prior to and after heat treatment.

	Without imprinting	Imprinted with DIMP	Imprinted with DEHMP
Before heat treatment	167 ± 10	173 ± 10	148 ± 10
Following heat treatment	126 ± 10	160 ± 10	148 ± 10

Table 2
Atomic percentage of various atoms as measured for DEHMP-imprinted TiO_2 by XPS in surface mode and in bulk mode.

	Bulk mode		Surface mode	
	Before heat treatment (at.%)	After heat treatment (at.%)	Before heat treatment (at.%)	After heat treatment (at.%)
O 1s	59.8	64.3	57.8	61.6
Ti 2p	18.1	19.2	16.0	18.7
C 1s	14.6	8.6	20.1	14.0
S 2p	5.7	6.1	4.7	5.1
P 2p	1.8	1.8	1.4	0.6
O:Ti ratio	3.3	3.3	3.6	3.3

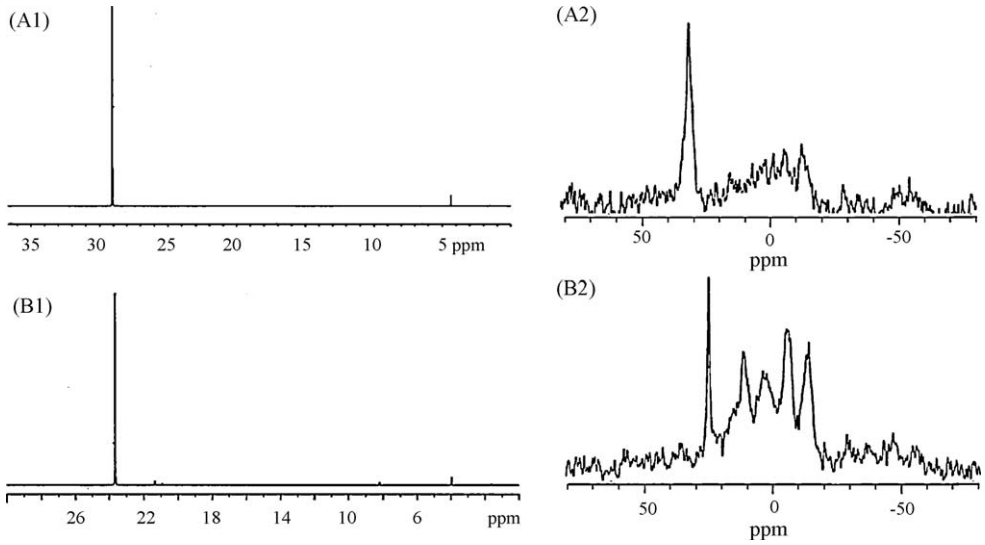

Fig. 5. ^{31}P NMR of TiO_2/phosphonates: (A1) liquid DIMP and (A2) imprinted DIMP on TiO_2 powder; (B1) liquid DEHMP and (B2) imprinted DEHMP on TiO_2 powder.

amounts to approximately 5 at.%, as well as from the appearance of typical [42,43] sulfate IR peaks at 1230 cm^{-1}, 1135 cm^{-1} and 1050 cm^{-1} upon performing KBr pellets FTIR measurements of the powder.

The interaction between the phosphonates and the TiO_2 matrix was studied by ^{31}P NMR. Here, liquid P NMR of DIMP and DEHMP as well as solid state P NMR of TiO_2/DIMP and TiO_2/DEHMP-imprinted powders were taken (Fig. 5A1–B2). The P NMR chromatograms of both liquid DIMP (A1) and powdered TiO_2/DIMP (A2) showed a single, well-defined peak at 29.1 ppm. This suggests that the phosphonate in the DIMP-imprinted TiO_2 was not covalently-attached to the titanium dioxide matrix. In contrast, a clear difference was observed between the P NMR of liquid DEHMP, which revealed a single peak at 23.6 ppm (B1), vs. that of DEHMP-imprinted TiO_2 powder (B2), where a combination of peaks at lower ppm, representing covalently-attached phosphonates, was observed together with the 23.6 ppm peak of the non-attached phosphonates. This difference between the two phosphonates is attributed to the DEHMP free hydroxyl, capable of interacting covalently with the TiO_2 surface.

3.2. Degradation experiments

The photocatalytic degradation of the two target molecules, DIMP and DEHMP, was studied with films consisting of titanium dioxide particles formed by the low-temperature titanyl sulfate method, with and without imprinting. Two control tests were carried out. The first comprised of monitoring the reactor chamber in the absence of light, while the second comprised of exposing the reactor cells containing heat-treated imprinted photocatalysts, but without any contaminant. In both cases there was no indication for the occurrence of any reaction.

3.2.1. The kinetics of DIMP degradation

Fig. 6 presents the evolution of the IR spectra during the photocatalytic degradation of DIMP in non-imprinted (A) and imprinted (B) photocatalysts. Typical DIMP peaks are observed at 917 cm^{-1}, 996 cm^{-1}, 1108 cm^{-1}, 1263 cm^{-1} and 2987 cm^{-1}, however, these peaks are difficult to observe due to the semi-volatility of the reactant and to its adsorption on the reactor's walls [10]. From the figure, it is evident that for both imprinted and non-imprinted photocatalysts, the photocatalytic degradation of DIMP involves the formation and destruction of acetone, noticed by its 1735 cm^{-1}, 1367 cm^{-1}, 1212 cm^{-1} IR peaks to yield CO_2 (2348 cm^{-1}) and water. The same scenario was observed in the past for the photocatalytic degradation on sol–gel made titanium dioxide [10]. Small amounts of CO (2178 cm^{-1} and 2119 cm^{-1}) were noticed during the photodegradation over molecular imprinted substrate. In addition, very weak peak, assigned to methane [44], was observed at 1304 cm^{-1}. It is noteworthy that residues of the phosphonates were not observed in the IR spectra suggesting that the phosphonate residues remained on the photocatalyst.

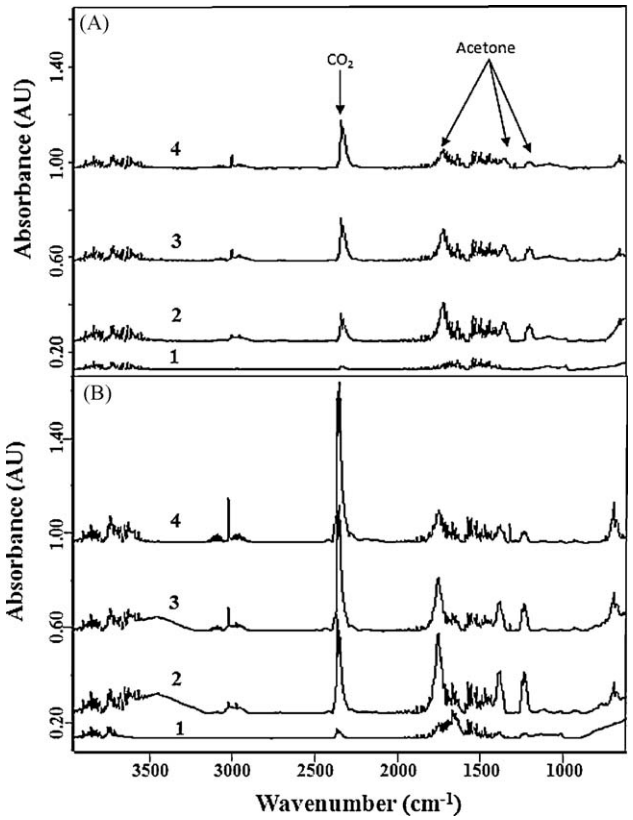

Fig. 6. The evolution of the FTIR spectrum measured upon photodegradation of DIMP on non-imprinted TiO_2 substrate (A) and DIMP-imprinted TiO_2 (B), before UV exposure (1) and following 20 h, 70 h, and 190 h of UV exposure (2, 3, 4, respectively). For clarity, the spectra are vertically shifted.

The effect of the imprinted sites on the photodegradation of DIMP is portrayed in Fig. 7A, which shows the kinetics of CO_2 formation for both types of substrates, deduced from the area of the CO_2 peak at 2348 cm^{-1}. As shown in the figure, the production rate of CO_2 in the presence of the imprinted sites was higher than the rate observed with samples of TiO_2 without imprinted sites by a factor of 3.2.

Acetone is an intermediate in the photodegradation process of DIMP [10]. Fig. 7B shows the kinetics of evolution and degradation of acetone, based on the area of the acetone-related ν(CO) peak at 1735 cm^{-1}. The maximal concentration of acetone was higher in the case of imprinted TiO_2, indicating faster degradation of DIMP with the imprinted TiO_2. In principle, the higher concentration of the intermediate product acetone could have been due to either faster degradation of DIMP or slower degradation of acetone. The post-maximal curves in Fig. 6B were fitted to exponentially decaying kinetics ($R^2 = 0.97$), indicating a pseudo first order kinetics. The pseudo rate constants were calculated as 0.0047 min^{-1} and 0.0051 min^{-1} with non-imprinted and imprinted particles, respectively. The similarity between these values suggests that the degradation rate of acetone is basically similar for the two cases. Hence, it can be concluded that the observed higher concentration of acetone at the maximal points was due to faster degradation of DIMP, rather than due to slower degradation of acetone. It can further be concluded that the DIMP-imprinted sites affect the degradation of DIMP but are ineffective in promoting the degradation of acetone.

It is noteworthy that the BET surface area of TiO_2 samples with imprinted sites was higher by factor of not more than 1.28 than that of the non-imprinted samples (160 m^2/g vs. 126 m^2/g), therefore one can deduce that the increased rate in the photocatalytic degradation of DIMP cannot be considered as due to the difference in the surface area.

3.2.2. The kinetics of DEHMP degradation

Fig. 8 presents the evolution of the IR spectra measured during the photocatalytic degradation of DEHMP with non-imprinted (A) and imprinted (B) substrates. A relatively strong carbonyl stretch peak is observed at 1740 cm^{-1}. This peak could have been assigned to the formation of acetone, nevertheless the absence of δ(CH) and ν(CC) peaks at 1367 cm^{-1} and 1212 cm^{-1}, respectively, negates this possibility. Other intermediate products are noticed in the spectra. An ethylene band is observed at 949 cm^{-1} and a C–O stretch of a primary alcohol is observed at 1054 cm^{-1}. Weak bands located at 1304 cm^{-1} and 2822 cm^{-1} can be assigned to methane and to a methoxy [45] group, respectively. Another bands, located at 2075 cm^{-1} and 2731 cm^{-1}, can be attributed to the C–H stretch mode of an aldehyde. A growth in CO concentration (2178 cm^{-1} and 2119 cm^{-1}) is noticed as well.

Fig. 9 presents the relative concentration of various chemical species identified while measuring the IR signal during the photocatalytic degradation of DEHMP on photocatalysts prepared with and without DEHMP imprinting. Fig. 9B presents the integrated absorbance of the 2731 cm^{-1} peak, assigned to C–H stretch mode of an aldehyde. A clear rise and fall of the aldehyde concentration as a function of time are observed for both types of substrates, indicating that the aldehyde is an intermediate product. Another peak showing an intermediate product behavior was that of the carbonyl group (1740 cm^{-1}, not shown here). It is noteworthy that the time of maximal concentrations of aldehydes and carbonyls was shorter with the imprinted samples than with non-imprinted samples. Based on well-known kinetics models this can serve as an indication for faster degradation kinetics of DEHMP upon using imprinted photocatalyst.

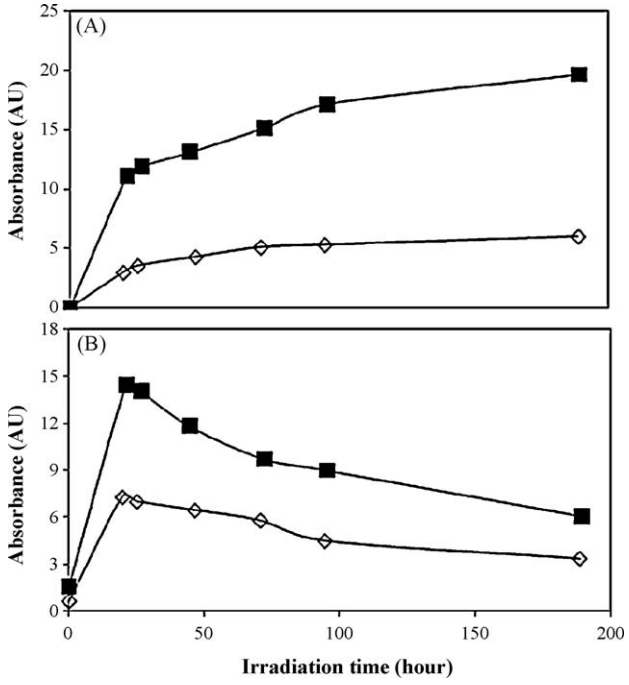

Fig. 7. Kinetics measured during the photodegradation of DIMP on DIMP-imprinted substrate (■) and on non-imprinted substrate (◇). The kinetics of (A) CO_2 production and (B) production and degradation of acetone.

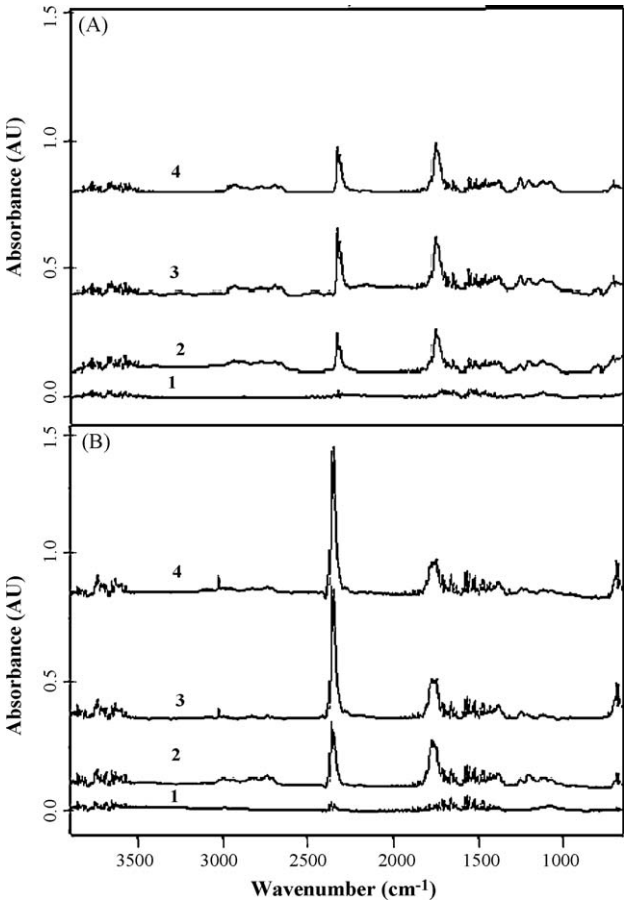

Fig. 8. The evolution of the FTIR spectrum measured upon photodegradation of DEHMP on non-imprinted TiO_2 substrate (A) and DEHMP-imprinted TiO_2 (B), before UV exposure (1) and following 15 h, 44 h, and 68 h of UV exposure (2, 3, 4, respectively). For clarity, the spectra are vertically shifted.

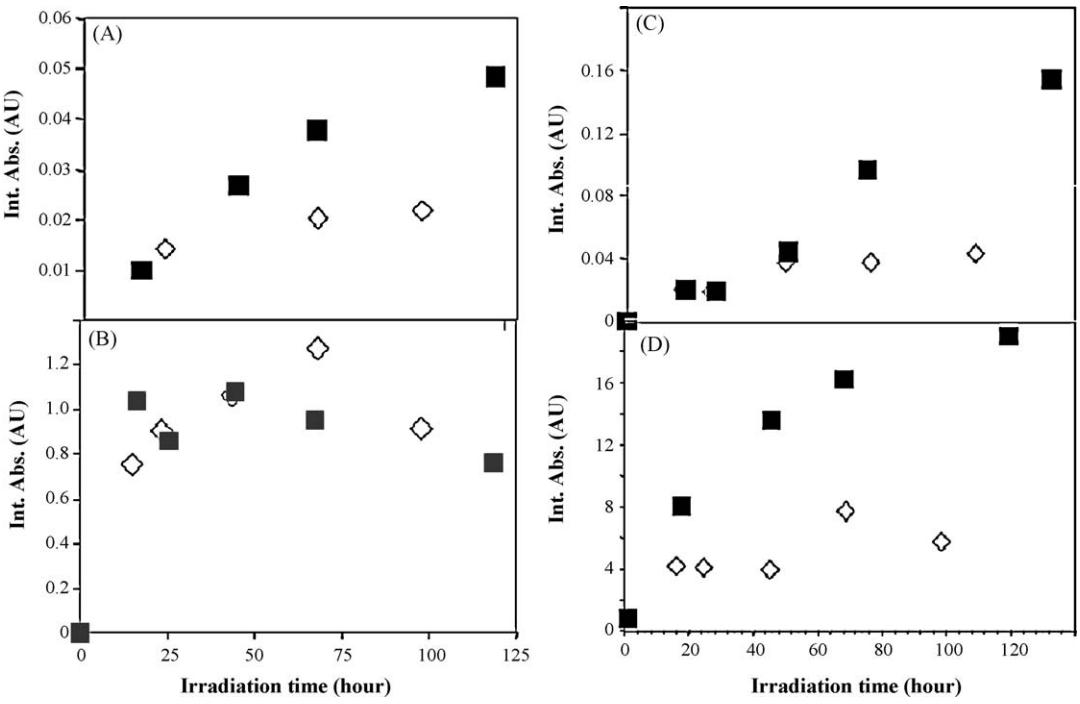

Fig. 9. The relative concentrations of intermediate products and end-products during the photocatalytic degradation of DEHMP on DEHMP-imprinted substrates (empty diamonds) and on non-imprinted substrates (filled squares). (A) Ethylene (949 cm^{-1}); (B) aldehyde, C–H stretch (2700 cm^{-1}); (C) methane (1304 cm^{-1}); (D) CO_2 (2348 cm^{-1}).

Three compounds whose concentrations were monotonically growing (hence can be regarded as end-products under the experimental conditions) were ethylene, methane and carbon dioxide. The integrated absorbance of their 949 cm^{-1}, 1304 cm^{-1} and 2348 cm^{-1} peaks, respectively, is depicted in Fig. 9A, C and D, respectively. For these three end-products, the production rate with the imprinted substrates was 2–3 times higher than with non-imprinted substrates. Some lag-time was observed in the production of methane, which may be explained by the methane being produced from intermediate products such as CH_3–O– or/and CH_3CH_2–O–. Some support, alas not definitive, could be obtained based on the growth pattern of a 1054 cm^{-1} peak, assigned to a primary alcohol (not shown here).

The BET surface area of DEHMP-imprinted TiO_2 samples was higher by a factor of 1.19 (149 m^2/g vs. 125 m^2/g), yet the production ratio of CO_2 (which was the main end-product) was 3.2 times higher. Hence, similar to the DIMP case, it can be deduced that the enhancement in the photocatalytic degradation of DEHMP was mainly due to the specific imprinting and not due to common surface area enhancement.

3.2.3. The kinetics of DIMP degradation over DEHMP-imprinted TiO_2

DIMP and DEHMP are very similar molecules. They differ in their hydrophobic tails (isopropyl vs. ethyl, respectively). More significantly, they differ in their R1 group attached to the phosphorous, namely methyl vs. methanol, respectively. The OH group in the DEHMP facilitates chemical bonding with the matrix, as portrayed in Fig. 2. It is for this reason that we found it interesting to study the photocatalytic degradation of DIMP using DEHMP-imprinted TiO_2.

TiO_2 particles, imprinted with DEHMP as described above, were produced. Following the preparation step the target molecules were removed by heat treatment, to form the imprinted molecular sites. The photocatalytic degradation of DIMP on this substrate was studied as described above and compared with that of non-imprinted substrates.

The FTIR spectra during the photocatalytic degradation of DIMP on DEHMP cavities were very similar to that obtained without cavities or with DIMP cavities, namely the formation of acetone (1735 cm^{-1}, 1367 cm^{-1}, 1212 cm^{-1}) as the only intermediate and carbon dioxide and water as end-products. No other intermediate or end-products were observed. As expected, we did not observe any peaks related to DEHMP degradation, indicating that the removal of the imprinting molecules during the heat treatment was complete.

Fig. 10 presents the CO_2 evolution with DEHMP-imprinted photocatalyst and with non-imprinted photocatalyst. Evidently, the production of CO_2 with the imprinted photocatalyst was by far faster than that with the non-imprinted photocatalyst. In fact, the mineralization ratio between the two photocatalysts was as high as 4.2, i.e. higher than that with the DIMP-imprinted photocatalyst. It is suggested, albeit not proved, that the chemical bonding

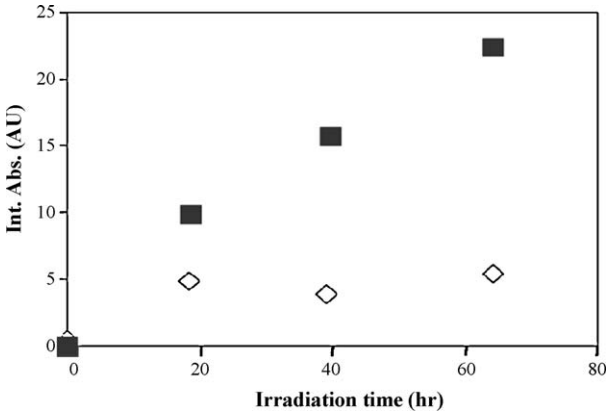

Fig. 10. The kinetics of CO_2 production as inferred from its 2348 cm^{-1} FTIR peak during the photocatalytic degradation of DIMP over DEHMP-imprinted TiO_2 (filled squares) and over non-imprinted TiO_2 (open diamonds).

between the imprinting molecule and the matrix helps to preserve the cavities. The fact that a homolog containing an appropriate chemical bonding group (an alcohol in this case) serves successfully as the imprinting molecule may provide a route for further investigation. It further points to the possibility of preparing a specially designed sarin-degrading photocatalyst without the need to use the highly toxic sarin as the imprinting molecule.

3.2.4. The kinetics of photocatalytic degradation of heptane over DIMP-imprinted TiO_2

The photocatalytic degradation of heptane over DIMP-imprinted TiO_2 was studied, and compared with that over non-imprinted TiO_2. The FTIR spectrum of heptane is very simple and contains a C–H stretch envelope at 2800–3000 cm^{-1} (with 2967 cm^{-1}, 2938 cm^{-1}, 2880 cm^{-1}, 2869 cm^{-1} peaks, corresponding to the asymmetric and the symmetric modes of the methyl and methylene groups) as well as weaker bands at 1465 cm^{-1} and 1385 cm^{-1}. For both substrates a decrease in the heptane-related peaks was clearly noticed, without the appearance of any (IR-active) intermediate products, and with carbon dioxide and water vapor as end-products.

Fig. 11A presents the integrated absorbance of the C–H stretch band of heptane, as measured in the reaction vessel, as a function of UV exposure time. Apparently, the disappearance of the heptane signal is of first order, revealing the same rate constant with the two substrates. In contrast, the CO_2 production, deduced from the same spectra, was found to be different for the two substrates. Here, the carbon dioxide production was higher with the imprinted substrates (Fig. 11B). The discrepancy between the graphs requires an explanation. The possibility that the excess of CO_2 observed with the imprinted substrates was due to incomplete removal of the imprinting (DIMP) molecules can be negated based on the small amount of imprinting molecules as well as based on the lack of gas phase acetone that is easily recognized as an intermediate

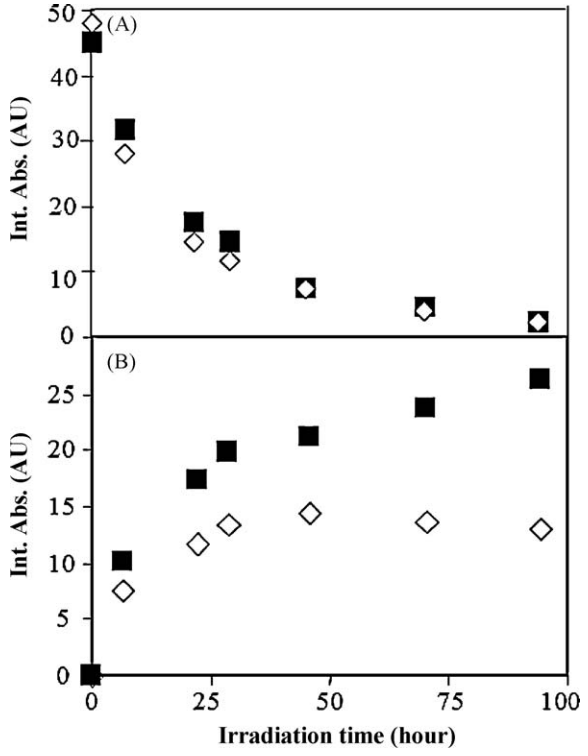

Fig. 11. The kinetics of the photocatalytic degradation of heptane over DIMP-imprinted TiO_2 (filled squares) and over non-imprinted TiO_2 film (open diamonds). (A) The integrated absorbance of the (A) C–H stretch mode of heptane at 2938 cm^{-1} and (B) CO_2 peak at 2348 cm^{-1}.

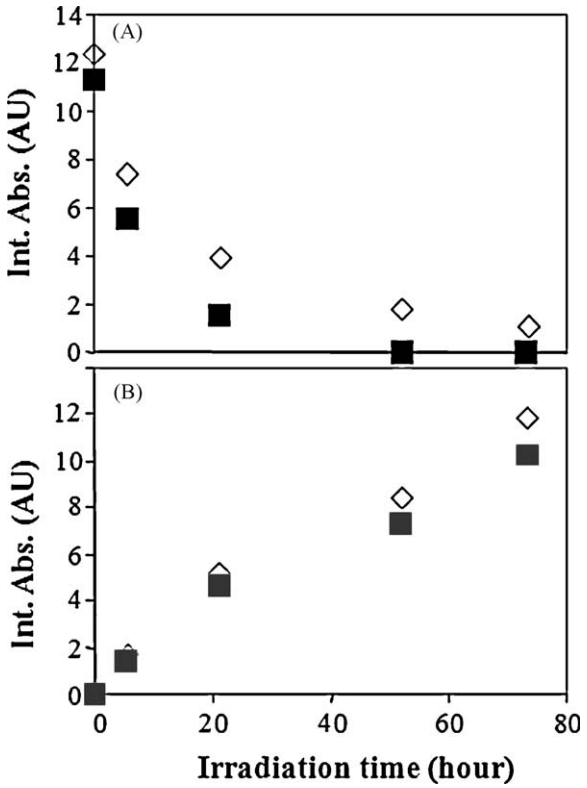

Fig. 12. The kinetics of photocatalytic degradation of benzene over DEHMP-imprinted substrate (filled squares) and over non-imprinted substrates (empty diamonds) as inferred from the integrated absorbance of the FTIR peaks during exposure. (A) The C–H aromatic stretch of benzene (3050 cm^{-1}) and (B) CO_2 (2348 cm^{-1}).

whenever DIMP is photocatalytically degraded. Likewise, the fact that no intermediate products were identified in the spectra negates the possibility of several products whose sum together with carbon dioxide is equal for the two cases. A mechanism operating only on the non-imprinted substrates, which produces IR-inactive species is also unlikely. It is proposed, albeit without direct proof, that the source of discrepancy is the build-up of three-dimensional islands of the semi-volatile heptane adsorbed mainly on the surface of the non-imprinted substrates. At any case, the enhancement in the production of carbon dioxide upon degrading heptane with DIMP-imprinted substrates is small compared with the enhancement that was obtained when DIMP-imprinted substrates were used in order to degrade DIMP.

3.2.5. The kinetics of photocatalytic degradation of benzene over DEHMP-imprinted TiO_2

The photocatalytic degradation of benzene by phosphonates-imprinted substrates was studied using FTIR by the same manner as described before. Upon exposure, a simultaneous decrease in all the typical peaks of benzene, namely the C–H aromatic stretch (3050 cm^{-1}), the C–C aromatic stretch (1482 cm^{-1}), the in-plane C–H bending (1037 cm^{-1}) and the out of-plane C–H bending (672 cm^{-1}) was observed. In parallel, a growth in the carbon dioxide peak was observed. No intermediate products or any other products except for carbon dioxide could be recognized. Fig. 12 describes the kinetics of degradation based on the integrated absorbance of the C–H aromatic stretch peak of benzene at 3050 cm^{-1} (A) and the CO_2 peak at 2348 cm^{-1} (B). According to Fig. 12A, the reduction in the benzene concentration was slightly faster with the imprinted substrates than with the non-imprinted, while the CO_2 production, deduced from the same set of

experiments (Fig. 12B), was slightly slower. Likewise, no effect of imprinting (in terms of benzene and CO_2 concentrations) was observed when the degradation of benzene with DIMP-imprinted substrates was compared to the photocatalytic degradation with non-imprinted substrates.

4. Discussion

Particles of titanium dioxide were synthesized at low temperatures with and without two imprinting molecules, DIMP and DEHMP. The particles were indexed as having the anatase phase, and the imprinting molecules were removed, to form the imprinted photocatalyst. It is evident that the introduction of the imprinting molecules induced higher photocatalytic degradation rates upon using films made from the imprinted particles. This higher degradation rate was manifested by a mineralization rate which was approximately 3–4 times higher than with non-imprinted substrates. This enhancement cannot be explained by the modest growth in the BET surface area connected with imprinting, as the difference in the surface area was no more than 20–30%. This conclusion is further supported by the lack of enhancement upon degrading benzene, as well as the lower extent of mineralization rate enhancement when the target molecule was heptane.

As mentioned above there were no indications for the appearance of (FTIR active) products containing phosphorous, in line with previously reported works on the photocatalytic degradation of DIMP [10]. In the case of photocatalytic oxidation of dimethyl methylphosphonate (DMMP), the obtained phosphor residues included methylphosphonic acid and phosphate. It was further found that these residues had a de-activation effect, which could be overcome easily by washing with water [46]. Although the surface of the photocatalyst was not analyzed in detail it is sensible to assume that these (or similar) non-volatile compounds were produced in the present study as well. Recently, it was reported that the presence of phosphor (on the surface or within the particles), may have a beneficial effect on photocatalytic rates [47]. Hence, it is legitimate to ask whether the observed increase in the photocatalytic rate was simply due to the presence of phosphor on the surface. For various reasons, the obtained data seem to disagree with such assumption. If this was the case, one could have expected that the difference in rates between the imprinted and the non-imprinted will be diminished as the reaction proceeded, since the degradation on both substrates had to produce phosphor compounds that remain on the surface. Furthermore, if the increased rate was due to surface phosphor that remained on the surface during preparation, then one could have expected to get faster kinetics with the imprinted samples regardless of the type of contaminant.

The presence of carbon on the surface of heat- treated imprinted samples might raise a question whether some organic phosphonates survived the high temperature heat treatment, in a manner that they later contributed to the higher degradation rates with the imprinted catalysts. The fact that imprinted samples that were exposed to UV light in the absence of gas phase reactants did not yield any products negates this possibility. Likewise, the degradation of DIMP on a photocatalyst containing DEHMP cavities did not yield any byproducts or end-products that could have been assigned to DEHMP. Besides, an evaluation of the amount of carbon that was left on the surface reveals that it was too small to have a significant effect on CO_2 production.

It can be concluded that the reported observations resulted from the conformity between the target molecules and the molecular cavities on the imprinted sites that facilitated the adsorption of the model contaminants. Another supportive evidence for the preferential way by which the imprinted sites operate is inferred from the photocatalytic degradation of acetone, an intermediate product of DIMP, where similar rate constants were obtained with the two types of substrates.

Of particular interest is the fact that substrates that were imprinted with DEHMP were found to be very effective in photocatalytically degrading the homolog DIMP. The alcohol group in DEHMP facilitates the formation of chemical bonds with the nascent titanium dioxide, as manifested by the ^{31}P NMR measurements. One may assume that good affinity between the host and the guest can play a major role in obtaining surfaces containing large concentration of separated, non-aggregated, imprinting molecules. Hence, the observation that DIMP degrades well on DEHMP-imprinted substrates suggests the use of molecules having good affinity to the matrix as a means to obtain high surface concentration of sites that are adequate for the degradation of their homolog molecules. This way, one can detour the problem of imprinting molecules that tend to aggregate due to inefficient affinity with the matrix. Another benefit is the possibility of using non- (or less) toxic homolog molecules for constructing the imprinted photocatalyst. This benefit is in particular important when designing a photocatalyst for WMD warfare agents, as in the case of sarin.

The approach described in this work is very versatile and can be used with large number of molecules. For example it can serve in tandem with biological treatment to get rid of highly toxic molecules that cannot be treated by the activated sludge approach. The imprinting approach can be further improved simply by overcoating thin layers of imprinted surfaces onto highly performing commercial photocatalysts, or, otherwise, by blocking all the non-imprinted parts of the surface, in a manner that may channel the photoinduced charge carriers towards the imprinted sites. Research in this direction is currently under work in our laboratory.

Acknowledgment

This work was supported by the Technion's VPR fund.

References

[1] Y. Paz, C. R. Chim. 9 (2006) 774–787.
[2] R.W. Matthews, Water Res. 20 (1986) 569–578.
[3] M.A. Fox, M.T. Dulay, Chem. Rev. 93 (1993) 341–357.
[4] L. Yezek, L.R. Rowell, M. Larwa, E. Chibowski, Colloids Surf. A: Physicochem. Eng. Aspects 141 (1998) 67–72.
[5] T. Rajh, O. Makarova, M.C. Thurnauer, P.A. Kemme, D. Cropek, 222nd ACS Meeting, Chicago, IL, 2001.
[6] S. Ghosh-Mukerji, H. Haick, M. Schvartzman, Y. Paz, J. Am. Chem. Soc. 123 (2001) 10776–10777.
[7] H. Haick, Y. Paz, J. Phys. Chem. B 105 (2001) 3045–3051.
[8] E. Zemel, H. Haick, Y. Paz, J. Adv. Oxid. Technol. 5 (2002) 27–32.
[9] S. Ghosh- Mukerji, H. Haick, Y. Paz, J. Photochem. Photobiol. A 160 (2003) 77–85.
[10] Y. Sagatelian, D. Sharabi, Y. Paz, J. Photochem. Photobiol. A 174 (2005) 253–260.
[11] F.H. Dickey, Natl. Acad. Sci. 35 (1949) 227–229.
[12] G. Vlatakis, L.I. Andersson, R. Muller, K. Mosbach, Nature 361 (1993) 645–647.
[13] B. Sellergren, Angew. Chem. 39 (2000) 1031–1037.
[14] B. Bjarnason, L. Chimuka, O. Ramstroem, Anal. Chem. 71 (1999) 2152–2156.
[15] B.R. Hart, J.K. Shea, Macromolecules 35 (2002) 6192–6201.
[16] L.I. Andersson, J. Chromatogr. B 739 (2000) 163–173.
[17] Z. Zhang, H. Liao, H. Li Hui, L. Nie, S. Yao, Anal. Biochem. 336 (2005) 108–116.
[18] G. Shustak, S. Marx, I. Turyan, D. Mandler, Electroanalysis 15 (2003) 398–408.
[19] C.M.F. Soares, G.M. Zanin, F.F. Moraes, d.-S. Andreo, A. Onelia, H.F. Castro, J. Inclus. Phenom. Macrocyclic Chem. 57 (2007) 79–82.
[20] K. Morihara, S. Kurihara, J. Suzuki, Bull. Chem. Soc. Jpn. 67 (1994) 1078–1084.
[21] A. Katz, M.E. Davis, Nature 403 (2000) 286–289.
[22] S.W. Lee, I. Ichinose, T. Kunitake, Langmuir 14 (1998) 2857–2863.
[23] I. Ichinose, T. Kikuchi, S.-W. Lee, T. Kunitake, Chem. Lett. (2002) 104–105.
[24] F. Dickert, O. Hayden, P. Lieberzeit, C. Palfinger, D. Pickert, U. Wolff, G. Scholl, Sens. Actuators B 95 (2003) 20–24.
[25] L. Feng, Y. Liu, J. Hu, Langmuir 20 (2004) 1786–1790.
[26] M. Lahav, A.B. Kharitonov, O. Katz, T. Kunitake, I. Willner, Anal. Chem. 73 (2001) 720–723.
[27] S. Huan, H. Chu, C. Jiao, G. Zeng, G. Huang, G. Shen, R. Yu, Anal. Chim. Acta 506 (2004) 31–39.

[28] C. Li, C. Wang, C. Wang, S. Hu, Sens. Actuators B 117 (2006) 166–171.
[29] C. Wang, C. Li, L. Wei, C. Wang, Microchim. Acta 158 (2007) 307–313.
[30] M.-J. Ju, D.-H. Yang, N. Takahara, K. Hayashi, K. Toko, S.-W. Lee, T. Kunitake, Chem. Commun. 25 (2007) 2630–2632.
[31] X. Shen, L. Zhu, H. Yu, H. Tang, S. Liu, W. Li, New J. Chem. 33 (2009) 1673–1679.
[32] X. Shen, L. Zhu, C. Huang, H. Tang, Z. Yu, F. Deng, J. Mater. Chem. 19 (2009) 4843–4851.
[33] Y. Zhang, R.L. Autenrieth, J.S. Bonner, S.P. Harvey, J.R. Wild, Biotechnol. Bioeng. 64 (1999) 221–231.
[34] O.P. Korobeinichev, A.A. Chernov, T.A. Bolshova, Combust. Flame 123 (2000) 412–420.
[35] E.J.P. Zegers, E.M. Fisher, Combust. Flame 115 (1998) 230–240.
[36] Y. Xie, B.N. Popov, Anal. Chim. Acta 448 (2001) 221–230.
[37] T.N. Obee, S. Satyapal, J. Photochem. Photobiol. A: Chem. 118 (1998) 45–51.
[38] J.A. Moss, S.H. Szczepankiewicz, E. Park, M. Hoffmann, J. Phys. Chem. B 109 (2005) 19779–19785.
[39] C.N. Rusu, J.T. Yates, J. Phys. Chem. B 104 (2000) 12292–12298.
[40] S. Yamabi, H. Imai, Thin Solid Films 434 (2003) 86–93.
[41] L. Jing, X. Sun, W. Cai, Z. Xu, Y. Du, H. Fu, J. Phys. Chem. Solids 64 (2003) 615–623.
[42] S. Ito, S. Inoue, H. Kawada, M. Hara, M. Iwasaki, H. Tada, J. Colloid Interface Sci. 216 (1999) 59–64.
[43] M. Iwasaki, M. Hara, S. Ito, J. Mater. Sci. Lett. 17 (1998) 1769–1771.
[44] J. Wu, S. Li, G. Li, C. Li, Q. Xin, Appl. Surf. Sci. 81 (1994) 37–41.
[45] J.-H. Wang, M.C. Lin, J. Phys. Chem. B 109 (2005) 20858–20867.
[46] T.N. Obee, S. Sunita, J. Photochem. Photobiol. A: Chem. 118 (1998) 45–51.
[47] D. Zhao, C. Chen, Y. Wang, H. Ji, W. Ma, L. Zang, J. Zhao, J. Phys. Chem. C 112 (2008) 5993–6001.